

# Phylloquinone (vitamin K<sub>1</sub>) biosynthesis in plants: two peroxisomal thioesterases of lactobacillales origin hydrolyze 1,4-dihydroxy-2-naphthoyl-coa

Joshua R. Widhalm<sup>1</sup>, Anne-Lise Ducluzeau<sup>1</sup>, Nicole E. Buller<sup>2</sup>, Christian G. Elowsky<sup>1</sup>, Laura J. Olsen<sup>2</sup> and Gilles J. C. Basset<sup>1\*</sup>

<sup>1</sup>Center for Plant Science Innovation, University of Nebraska-Lincoln, Lincoln, NE 68588, USA, and

<sup>2</sup>Department of Molecular, Cellular, and Developmental Biology, University of Michigan, Ann Arbor, MI 48109, USA

Received 2 May 2011; revised 19 January 2012; accepted 22 February 2012; published online 19 June 2012.

\*For correspondence (e-mail gbasset2@unl.edu).

## SUMMARY

It is not known how plants cleave the thioester bond of 1,4-dihydroxy-2-naphthoyl-CoA (DHNA-CoA), a necessary step to form the naphthoquinone ring of phylloquinone (vitamin K<sub>1</sub>). In fact, only recently has the hydrolysis of DHNA-CoA been demonstrated to be enzyme driven *in vivo*, and the cognate thioesterase characterized in the cyanobacterium *Synechocystis*. With a few exceptions in certain prokaryotic (*Sorangium* and *Opitutus*) and eukaryotic (*Cyanidium*, *Cyanidioschyzon* and *Paulinella*) organisms, orthologs of DHNA-CoA thioesterase are missing outside of the cyanobacterial lineage. In this study, genomic approaches and functional complementation experiments identified two *Arabidopsis* genes encoding functional DHNA-CoA thioesterases. The deduced plant proteins display low percentages of identity with cyanobacterial DHNA-CoA thioesterases, and do not even share the same catalytic motif. GFP-fusion experiments demonstrated that the *Arabidopsis* proteins are targeted to peroxisomes, and subcellular fractionations of *Arabidopsis* leaves confirmed that DHNA-CoA thioesterase activity occurs in this organelle. *In vitro* assays with various aromatic and aliphatic acyl-CoA thioester substrates showed that the recombinant *Arabidopsis* enzymes preferentially hydrolyze DHNA-CoA. Cognate T-DNA knock-down lines display reduced DHNA-CoA thioesterase activity and phylloquinone content, establishing *in vivo* evidence that the *Arabidopsis* enzymes are involved in phylloquinone biosynthesis. Extraordinarily, structure-based phylogenies coupled to comparative genomics demonstrate that plant DHNA-CoA thioesterases originate from a horizontal gene transfer with a bacterial species of the *Lactobacillales* order.

**Keywords:** *Arabidopsis*, chloroplast, hotdog-fold, peroxisome, phylloquinone, *Synechocystis*.

## INTRODUCTION

In plants and certain species of cyanobacteria, phylloquinone (2-methyl-3-phytyl-1,4-naphtho-quinone or vitamin K<sub>1</sub>; Figure 1a) is a vital redox co-factor required for electron transfer in photosystem I and the formation of protein disulfide bonds (Brettel *et al.*, 1986; Sigfridsson *et al.*, 1995; Singh *et al.*, 2008; Furt *et al.*, 2010; Karamoko *et al.*, 2011). A closely related form called menaquinone [2-methyl-3-(all-trans-polyprenyl)-1,4-naphthoquinone or vitamin K<sub>2</sub>] is synthesized by red algae, diatoms, and most archaeal and bacterial species (Collins and Jones, 1981; Yoshida *et al.*, 2003; Ikeda *et al.*, 2008). In vertebrates, vitamin K is needed for blood coagulation, bone and vascular metabolism, and signaling (Booth, 2009). For humans in particular, the phylloquinone of green leafy vegetables and vegetable oils, such

as that of *Glycine max* (soybean), *Helianthus annuus* (sunflower), *Olea europaea* (olive), and *Brassica sp.* (canola), is the main contributor of dietary vitamin K (Booth and Suttie, 1998).

Despite the importance of phylloquinone in photosynthesis and human nutrition, the molecular architecture of its biosynthesis in plants has only recently been explored. The immediate precursor of the redox active naphthoquinone ring of phylloquinone is chorismate (Figure S1). It is first isomerized to serve as a substrate for an atypical multifunctional enzyme, termed PHYLLLO, that catalyzes sequential steps of addition, elimination and aromatization, suggestive of a channeling mechanism (Gross *et al.*, 2006). The product from PHYLLLO, *o*-succinylbenzoate, is

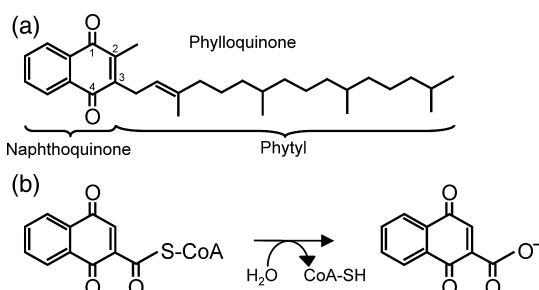


**Figure 1.** Structure of phylloquinone and the DHNA-CoA thioesterase catalyzed reaction.

(a) The phylloquinone molecule is bipartite, comprising a redox-active naphthoquinone ring and a liposoluble phytyl side chain.

(b) The hydrolysis of DHNA-CoA frees the carboxyl group of DHNA for its subsequent phytylation.

then activated by ligation with CoA and cyclized, yielding the CoA thioester of 1,4-dihydroxy-2-naphthoate (DHNA). DHNA-CoA is subsequently hydrolyzed, and DHNA is prenylated and methylated (Shimada *et al.*, 2005; Lohmann *et al.*, 2006; Kim *et al.*, 2008). In agreement with radiolabeling assays showing that the prenylation and methylation reactions are associated with plastidial membranes (Schultz *et al.*, 1981; Gaudillière *et al.*, 1984; Kaiping *et al.*, 1984), several enzymes involved in the formation of the naphthoquinone ring and its subsequent conjugation to the phytyl moiety have been shown to occur in the chloroplast (Shimada *et al.*, 2005; Gross *et al.*, 2006; Lohmann *et al.*, 2006; Strawn *et al.*, 2007; Garcion *et al.*, 2008; Kim *et al.*, 2008). This apparent all-plastidial localization of the phylloquinone biosynthetic pathway has nevertheless recently been challenged by proteomic studies that identified homologs of prokaryotic DHNA-CoA synthase in *Arabidopsis* and *Spinacia oleracea* (spinach) peroxisomal fractions (Reumann *et al.*, 2007; Babujee *et al.*, 2010). GFP-reporter experiments and detection of consensus targeting signals not only confirmed the finding, but also showed that the preceding enzyme – OSB-CoA ligase – is probably dual targeted to peroxisomes and plastids (Kim *et al.*, 2008; Babujee *et al.*, 2010). Although direct evidence that peroxisomal preparations actually display the aforementioned ligase and synthase activities is lacking, these preliminary results raise the intriguing possibility of a split of the phylloquinone biosynthetic pathway between chloroplasts and peroxisomes.

Besides such a fragmentary understanding of the enzymatic arrangement in plant phylloquinone biosynthesis, one step in the pathway – the hydrolysis of DHNA-CoA (Figure 1b) – remains unidentified. In fact, the cleavage of the thioester bond of DHNA-CoA has long been an enigma in both prokaryotic and eukaryotic vitamin K-synthesizing organisms. Forward-genetics strategies failed to isolate any mutants related to this step, and given the propensity of

DHNA-CoA to spontaneously hydrolyze at physiological pH levels, it seemed *a priori* plausible that such a reaction was non-specific (Sakuragi and Bryant, 2006). Only recently was a dedicated DHNA-CoA thioesterase identified in the cyanobacterium *Synechocystis* PCC 6803 using a combination of phylogenomics and reverse-genetics approaches (Widhalm *et al.*, 2009). The enzyme, which appeared to have evolved an absolute substrate specificity for DHNA-CoA (Widhalm *et al.*, 2009), was found to be related to the 4-hydroxybenzoyl-CoA thioesterase (4HBT) family of hotdog-fold proteins (Dillon and Bateman, 2004). Relying exclusively on sequence homology to identify non-cyanobacterial DHNA-CoA thioesterase orthologs turns out to be problematic, because 4HBT-like enzymes are notorious for displaying low levels of overall sequence conservation, and even dissimilar active sites, while bearing similar substrate specificity (Cantu *et al.*, 2010). Typical examples are *Pseudomonas* and *Arthrobacter* 4HBTs that catalyze the same reaction in the degradation pathway of 4-chlorobenzoate, but are classified in two separate phylogenetic subfamilies having distinct catalytic residues and quaternary structures (Benning *et al.*, 1998; Thoden *et al.*, 2002; Cantu *et al.*, 2010).

In this study, we identified two *Arabidopsis* members of the 4HBT family encoding highly specific DHNA-CoA thioesterases that are targeted to peroxisomes and participate in phylloquinone biosynthesis. Using phylogenetic reconstructions, we show that these plant enzymes are not orthologous to cyanobacterial DHNA-CoA thioesterase, and probably originate from a lateral gene transfer from a bacterium of the *Lactobacillales* order.

## RESULTS

### **Arabidopsis genes *At1g48320* and *At5g48950* encode for members of the 4HBT family that fully complement *synechocystis* DHNA-CoA thioesterase knock-out**

Searching the Pfam database of protein families (Finn *et al.*, 2010) for entries containing a predicted 4HBT domain identified 12 hotdog-fold proteins in *Arabidopsis*. Cognate full-length cDNAs were obtained for all of them, except the putative product of gene *At1g68280* (see the Experimental procedures). Mining expressed sequence tag and microarray databases did not detect any hits for *At1g68280* either. Analysis of the genomic context of *At1g68280* showed that this gene actually occurs as a tandem repeat of gene *At1g68260* (the corresponding deduced proteins being 83% identical), indicative of a recent event of gene duplication. Because such features typify *At1g68280* as a pseudogene, it was not investigated further. The other 11 cDNAs were individually subcloned into expression vector pSynExp-2 under the control of the cyanobacterial *psbA2* promoter (Sattler *et al.*, 2003) and introduced into *Synechocystis* strain *Δslr0204*. This strain is a DHNA-CoA thioesterase

knock-out that lacks phyloquinone and is photosensitive (Widhalm *et al.*, 2009). Out of the 11 aforementioned cDNAs, two corresponding to genes *At1g48320* and *At5g48950* restored cell growth at high-light intensities, as did the reintroduction of gene *Slr0204*, providing initial genetic evidence for the existence of functional plant DHNA-CoA thioesterases (Figure 2a). The deduced *At1g48320* and *At5g48950* proteins share 63% identity and 78% similarity, indicating that they are likely paralogs. Remarkably, each of these Arabidopsis proteins shows low percentages of homology (approximately 15% identity/approximately 30% similarity) with *Synechocystis* Slr0204. Only cells expressing the *At1g48320*, *At5g48950* and endogenous *Slr0204* proteins displayed phyloquinone levels similar to that of the wild-type reference strain (Figure 2b). The *At1g48320* and *At5g48950* proteins, previously named small thioesterase ST1 and ST2, respectively (Reumann *et al.*, 2009), were re-named for this study *Arabidopsis thaliana* DHNA-CoA

thioesterase 1 and 2, respectively (abbreviated hereafter as AtDHNAT1 and AtDHNAT2).

#### AtDHNAT1 and AtDHNAT2 occur in peroxisomes, and so does DHNA-CoA thioesterase activity

AtDHNAT1 and AtDHNAT2 both have C-terminal tripeptides (AKL and SKL, respectively), typifying peroxisomal targeting signals type 1 (Reumann, 2004a), and are *de facto* listed in the AraPero database of putative proteins of Arabidopsis peroxisomes (<http://www3.uis.no/araperoxv1>; Reumann *et al.*, 2004b). Similarly, a survey of the TAIR database (<http://www.arabidopsis.org/index.jsp>) confirmed that signature fragments of AtDHNAT1 have been identified through large-scale proteomic experiments in purified peroxisomes, and that the N-terminally eYFP-tagged protein is targeted to this organelle (Reumann *et al.*, 2009). To verify the subcellular localization of AtDHNAT2, its full-length cDNA was fused to the C-terminal end of GFP. Co-expression of this fusion protein with an RFP-tagged peroxisomal marker resulted in a distinctive punctate pattern and co-localization of the green and red pseudocolors in peroxisomes (Figure 3a,b,d). No GFP-associated fluorescence was observed in plastids (Figure 3c,d). To confirm these findings, chloroplasts, mitochondria and peroxisomes were isolated from Arabidopsis leaves, using assays of marker enzymes to monitor the integrity and enrichment of each organelle preparation (Table 1). Of the three purified organelles, DHNA-CoA thioesterase activity was detected only in peroxisomes (Table 1). Enrichment and recovery of DHNA-CoA thioesterase activity (approximately threefold and approximately 2%, respectively) were similar to those of catalase (approximately fivefold and approximately 2%, respectively). These data indicate that Arabidopsis DHNA-CoA thioesterase activity occurs in peroxisomes, but not in plastids and mitochondria, and coincides with the subcellular localization of AtDHNAT1 and AtDHNAT2.

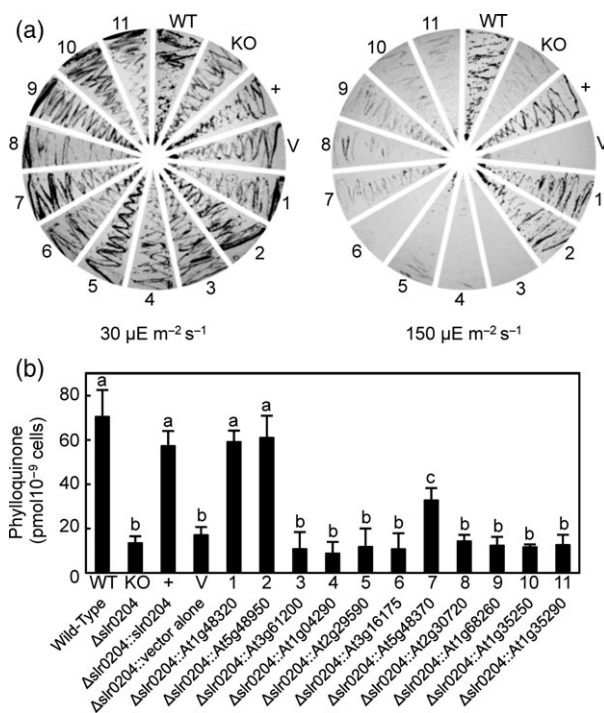


**Figure 2.** Identification of two Arabidopsis 4-HBT-like proteins that encode functional DHNA-CoA thioesterases.

(a) Functional complementation of *Synechocystis* DHNA-CoA thioesterase knock-out mutant ( $\Delta slr0204$ ). Similar number of cells of wild-type (WT), mutant (KO), and mutant transformed with vector alone (V) or native gene *Slr0204* (+) or Arabidopsis cDNAs encoding predicted 4-HBT domain-containing proteins (clones 1–11) were plated on BG-11 without glucose or antibiotics. Plates were incubated at 22°C for 2 weeks under low ( $30 \mu\text{E m}^{-2} \text{s}^{-1}$ ) or high ( $150 \mu\text{E m}^{-2} \text{s}^{-1}$ ) light intensities.

(b) HPLC-fluorescence quantification of phyloquinone in *Synechocystis* extracts. Clone nomenclature is the same as in panel (a). Data are means  $\pm$  SEs of three biological replicates. Columns with differing letter annotation are significantly different, as determined by Fisher's least significant difference test ( $P < \alpha = 0.05$ ) from an analysis of variance.

#### AtDHNAT1 and AtDHNAT2 display marked substrate preference for DHNA-CoA *in vitro*

To study the substrate specificity of AtDHNAT1 and AtDHNAT2, 6xhis-tagged versions were expressed in *Escherichia coli* and purified by affinity chromatography (Figure S2). The DHNA-CoA thioesterase-specific activities measured in crude extracts of clones harboring AtDHNAT1 and AtDHNAT2 were 8- and 38-fold higher than that of the control cell extract, respectively (Table S1).

The purified enzymes displayed comparable DHNA-CoA thioesterase specific activity to *Synechocystis* Slr0204 DHNA-CoA thioesterase assayed at a similar substrate concentration, i.e.  $74\text{--}118 \mu\text{mol h}^{-1} \text{mg}^{-1}$  for AtDHNAT1 and AtDHNAT2 at  $90 \mu\text{M}$  DHNA-CoA versus  $102 \mu\text{mol h}^{-1} \text{mg}^{-1}$  for Slr0204 at  $65 \mu\text{M}$  DHNA-CoA (Figure 4; Widhalm *et al.*, 2009). AtDHNAT2 also displayed activity towards

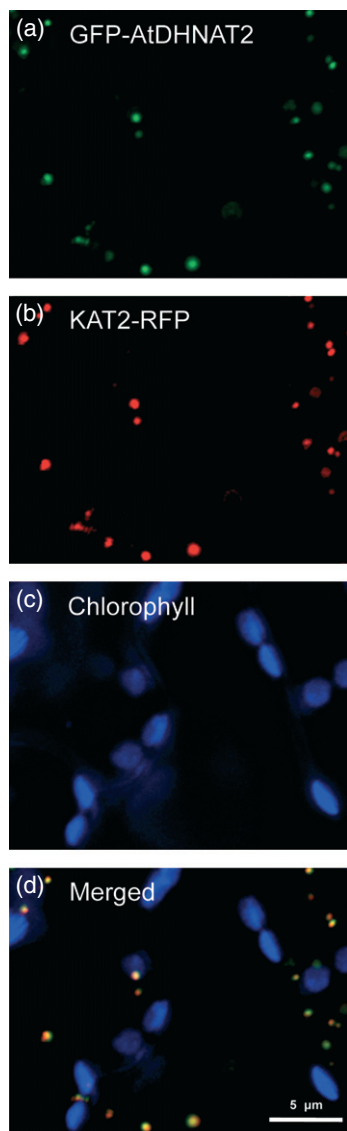


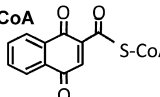
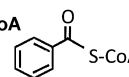
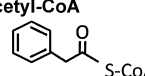
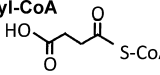
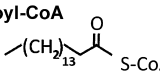
**Figure 3.** Subcellular localization of AtDHNAT2. (a) green pseudocolor of GFP-tagged AtDHNAT2. (b) red pseudocolor of peroxisomal marker RFP-tagged 3-keto-acyl-CoA thiolase 2 (KAT2; fragment 1–99). (c) blue pseudocolor of plastid autofluorescence. (d) overlay.

benzoyl-CoA, although the measured value was approximately an order of magnitude lower than that obtained with DHNA-CoA as the substrate (Figure 4). All the other activities measured with the aromatic acyl-CoA thioesters and the short-chain aliphatic acyl-CoA thioester succinyl-CoA were detected at trace levels (Figure 4). No activity was detected against the long-chain aliphatic acyl-CoA thioester palmitoyl-CoA (Figure 4). AtDHNAT1 and AtDHNAT2 thus appear to have marked substrate preference for DHNA-CoA, and in that regard resemble cyanobacterial DHNA-CoA thioesterase (Widhalm *et al.*, 2009).

**Table 1** Arabidopsis DHNA-CoA thioesterase activity co-purifies with peroxisomes

	$\mu\text{mol min}^{-1} \text{mg}^{-1} \text{protein}$			$\text{nmol h}^{-1} \text{mg}^{-1} \text{protein}$
	GAPDH	Fumarase	Catalase	DHNA-CoA thioesterase
CE	$0.93 \pm 0.1$	$0.41 \pm 0.03$	$55 \pm 15$	$2.4 \pm 0.52$
CP	$1.6 \pm 0.23$	$<0.01$	$9.8 \pm 1.4$	$<0.5$
MT	$<0.001$	$54 \pm 18.9$	$24 \pm 4.8$	$<0.5$
PX	$<0.001$	0.11	287	$7.3 \pm 0.3$

DHNA-CoA thioesterase and marker enzyme activities were assayed in crude extracts (CEs), stromal fraction of percoll-purified chloroplasts (CPs), matrix fraction of percoll-purified mitochondria (MT) and matrix fraction of percoll-purified peroxisomes (PXs) of Arabidopsis leaves. NADP-linked glyceraldehyde-3-phosphate dehydrogenase (GAPDH), fumarase and catalase were used as marker enzymes for chloroplasts, mitochondria and peroxisomes, respectively. Data are means of three biological replicates  $\pm$  SEs, except for the marker assays on peroxisomes, for which single measurements were performed.

Substrate [90 $\mu\text{M}$ ]	Specific activity ( $\mu\text{mol h}^{-1} \text{mg}^{-1} \text{protein}$ )	
	AtDHNAT1	AtDHNAT2
DHNA-CoA 	$74 \pm 21$	$118 \pm 23$
Benzoyl-CoA 	$1.2 \pm 0.48$	$15.1 \pm 4.7$
Phenylacetyl-CoA 	$0.48 \pm 0.2$	$0.53 \pm 0.2$
Succinyl-CoA 	$2.1 \pm 0.82$	$2.3 \pm 0.17$
Palmitoyl-CoA 	$< 0.001$	$< 0.001$

**Figure 4.** Substrate specificity of AtDHNAT1 and AtDHNAT2. Purified recombinant AtDHNAT1 and AtDHNAT2 (0.013–2.700  $\mu\text{g}$ ) were assayed with various aromatic and aliphatic acyl CoA-thioester substrates, all at the concentration of 90  $\mu\text{M}$ . DHNA-CoA thioesterase activity was monitored by direct quantification of DHNA using HPLC with diode array and fluorescence detection; the hydrolysis of the other substrates was measured spectrophotometrically by derivatization of free CoA-SH with the thiol-reagent DTNB. Data are means  $\pm$  SEs of three biological replicates.

#### AtDHNAT1 and AtDHNAT2 participate in phylloquinone biosynthesis in Arabidopsis

Two T-DNA lines from the SAIL collection (Sessions *et al.*, 2002) corresponding to insertions located in the first exon of



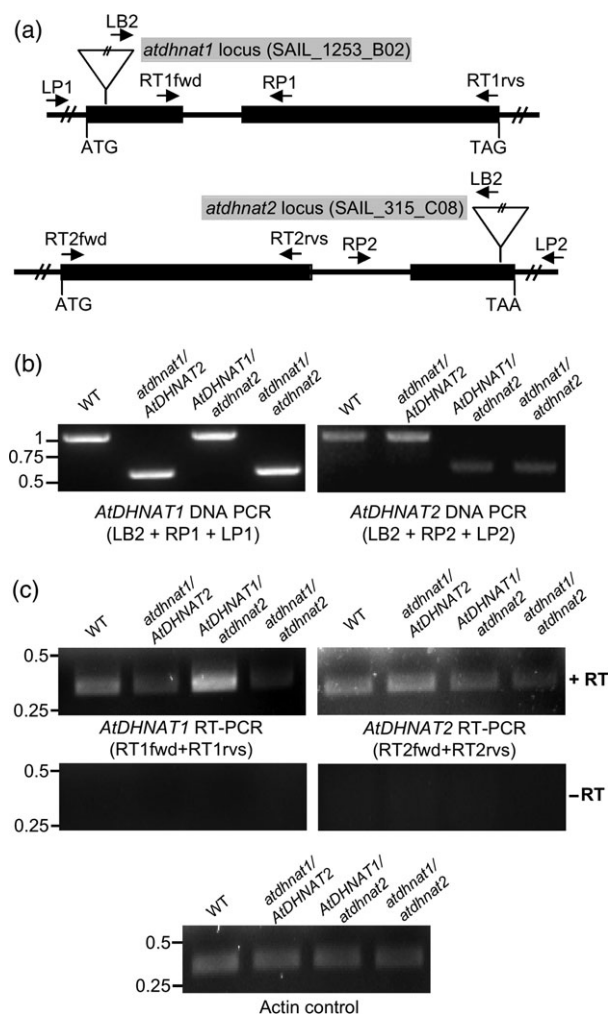


**Figure 5.** Molecular characterization of the *atdhnat1* and *atdhnat2* T-DNA mutants.

(a) Structure of the *AtDHNAT1* and *AtDHNAT2* genes, and location of their respective T-DNA insertions. Black boxes symbolize exons; joining lines symbolize introns. LP1 and LP2, RP1 and RP2, and LB2 indicate the location of the genotyping primers, whereas RT1 and 2fwd, and RT1 and 2rvs indicate that of the RT-PCR primers.

(b) Genotyping PCRs on wild-type Arabidopsis plants (WT) and T-DNA insertion lines corresponding to *AtDHNAT1* (*atdhnat1 AtDHNAT2*) and *AtDHNAT2* (*AtDHNAT1 atdhnat2*) single mutants and to the double mutant (*atdhnat1 atdhnat2*).

(c) Semi-quantitative RT-PCR analyses. –RT, controls for genomic DNA contamination performed without reverse transcriptase.

*AtDHNAT1* (SAIL\_1253\_B02) and in the second exon of *AtDHNAT2* (SAIL\_315\_C08) were identified, and confirmed by DNA genotyping (Figure 5a,b). Yet, RT-PCR experiments using primer pairs designed to amplify cDNA regions located after and before the T-DNA insertions of the *atdhnat1* and *atdhnat2* mutants, respectively (Figure 5a), demonstrated that none of these loci were null (Figure 5c). However, each insertion line displayed a marked reduction in DHNA-CoA thioesterase specific activity compared with

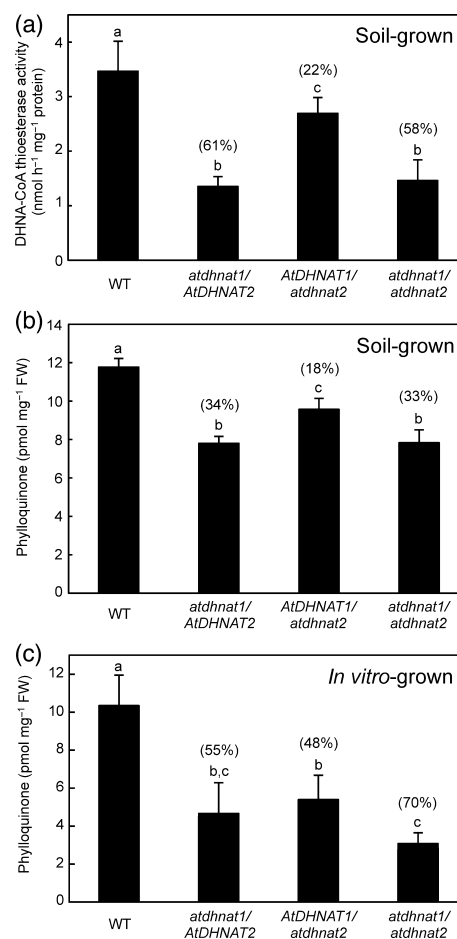


**Figure 6.** *AtDHNAT1* and *AtDHNAT2* knock-out mutants display reduced DHNA-CoA thioesterase activity and phyloquinone content.

(a) Desalted extracts of soil-grown wild-type and mutant Arabidopsis plants were assayed for DHNA-CoA thioesterase activity for 20 min at 30°C. Assays contained 85 μM DHNA-CoA and 21–49 μg of proteins.

(b) Phyloquinone levels in the leaves of wild-type and mutant Arabidopsis plants grown on soil.

(c) Same as in panel (b), but plants were grown on Murashige and Skoog medium containing 3% sucrose. Percentages in brackets indicate the reduction in DHNA-CoA thioesterase activity or phyloquinone content of each T-DNA line compared with wild-type plants. Data are means ± SEs of three biological replicates. Columns with differing letter annotation are significantly different, as determined by Fisher's least significant difference test ( $P < \alpha = 0.05$ ) from an analysis of variance.

wild-type controls, indicating that the *atdhnat1* and *atdhnat2* T-DNA loci are not fully functional (Figure 6a). The loss in DHNA-CoA thioesterase activity ranged from approximately 60% for *atdhnat1 AtDHNAT2* and *atdhnat1 atdhnat2*–22% for *AtDHNAT1 atdhnat2* (Figure 6a). The remaining DHNA-CoA thioesterase activity was found to still co-purify with peroxisomes in the double knock-down mutant (Table 2). Compared with wild-type plants, phyloquinone levels were reduced by 34 and 33% in *atdhnat1 AtDHNAT2* and *atdhnat1 atdhnat2*, respectively, and by 18% in *AtDHNAT1 atdhnat2* (Figure 6b). This reduction in phyloquinone content was

**Table 2** DHNA-CoA thioesterase activity in double knock-out mutant *atdhnat1 atdhnat2*

	$\mu\text{mol min}^{-1} \text{mg}^{-1} \text{protein}$			$\text{nmol h}^{-1} \text{mg}^{-1} \text{protein}$
	GAPDH	Fumarase	Catalase	DHNA-CoA thioesterase
CE	$0.53 \pm 0.0$	$0.30 \pm 0.06$	$40 \pm 19$	$1.87 \pm 1.07$
PX	$<0.01$	$0.14 \pm 0.03$	$113 \pm 6.4$	$4.67 \pm 0.84$

DHNA-CoA thioesterase and marker enzyme activities were assayed in crude extracts (CEs) and the matrix fraction of percoll-purified peroxisomes (PXs) from the leaves of the *Arabidopsis* double knock-out mutant *atdhnat1 atdhnat2*. Assays were as described in Table 1. Data are means of two biological replicates  $\pm$  SEs. Note that in this experiment, peroxisomes were not prepared with the same protocol as that used for Table 1 (see Experimental procedures). Absolute values of specific activities are therefore not comparable.

far more pronounced when the plants were grown *in vitro*, with levels being decreased by 55, 48 and 70% in *atdhnat1 AtDHNAT2*, *AtDHNAT1 atdhnat2* and *atdhnat1 atdhnat2*, respectively (Figure 6c). Neither of the corresponding homozygous mutants (*atdhnat1 AtDHNAT2* and *AtDHNAT1 atdhnat2*) nor the double homozygous mutant (*atdhnat1 atdhnat2*) differed phenotypically from wild-type plants (Figure S3).

#### Plant and cyanobacterial DHNA-CoA thioesterases belong to separate phylogenetic subfamilies

Because nothing is known about the evolutionary relationships of plant and cyanobacterial DHNA-CoA thioesterases, we reconstructed their phylogeny within families of related hotdog-fold CoA thioesterases. The bias in protein alignment resulting from the weak conservation of amino acid sequences in this class of enzymes (Cantu *et al.*, 2010) was corrected by superposing secondary structures and catalytic sites with those of hotdog-fold CoA thioesterases of solved crystal structures (Figure S4). These reference enzymes were selected as those for which experimental evidence for DHNA-CoA thioesterase activity exists, at least *in vitro* (*E. coli* YbdB; pdb file 1VH9; Jiang *et al.*, 2008), or for which DHNA-CoA thioesterase function could be robustly inferred from phylogenomics evidence (*Prochlorococcus marinus* Slr0204; pdb file 2HX5; Widhalm *et al.*, 2009). The alignment was then populated with the closest homologues from various prokaryotic and eukaryotic organisms. A structure of *E. coli* phenylacetic acid protein I (Paal; pdb file 2FS2) was also included, for *AtDHNAT1* and *AtDHNAT2* are classified in the NCBI and TAIR databases as Paal enzymes. The cognate tree establishes that plant and cyanobacterial DHNA-CoA thioesterases belong to strikingly different subfamilies (Figure 7a), the catalytic motif of which are even unrelated (Figure S4). Notably, three eukaryotic members from rhodophytes (red algae) and euglyphidae cluster within the

cyanobacterial subfamily (Figure 7a). These eukaryotic enzymes are plastid-encoded and, as occurs in present-day cyanobacteria, have genes organized in vitamin K biosynthetic clusters, pointing to a likely origin as remnants of cyanobacterial endosymbionts (Figure 7b). In stark contrast, *AtDHNAT1* and *AtDHNAT2*, and their homologues in monocots, gymnosperms, mosses and Lycopodiophytes, regroup monophyletically with eubacterial proteins of the *Lactobacillales* order (Figure 7a). Just as remarkable is the finding that the corresponding genes in multiple *Lactobacillales* and other firmicutes species occur in clusters of menaquinone biosynthetic genes, thus providing unequivocal evidence that these hotdog-fold proteins encode DHNA-CoA thioesterases (Figure 7b). Using the nomenclature proposed in the most recent classification of thioester-active enzymes (Cantu *et al.*, 2011), plant DHNA-CoA thioesterases therefore appear as members of the TE11/4HBT-II-type subfamily of CoA thioesterases, whereas their cyanobacterial counterparts represent a subfamily of their own (TE12/Slr0204-type). It is also evident that the prevailing annotation of plant DHNA-CoA thioesterases as part of the Paal/TE13 subfamily is erroneous.

#### DISCUSSION

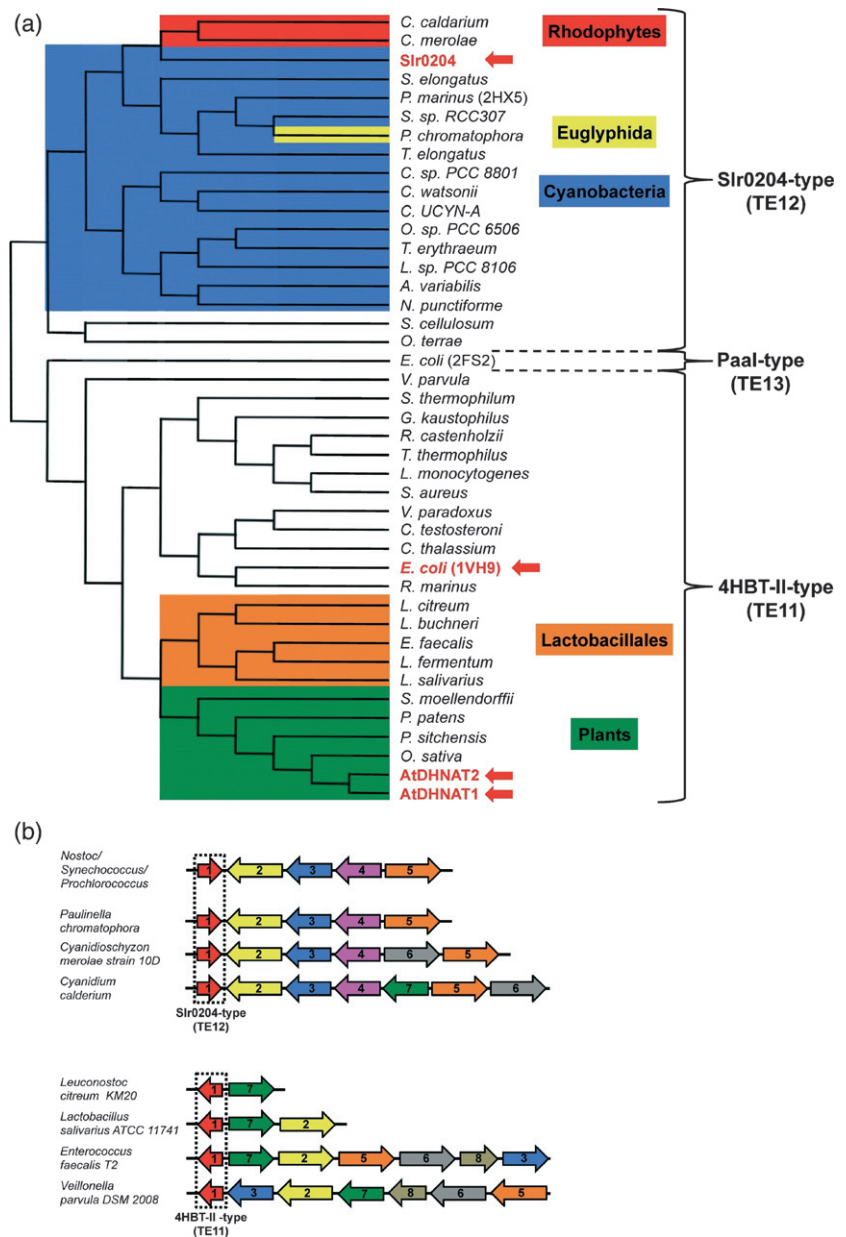
We have identified two *Arabidopsis* cDNAs specifying peroxisomal DHNA-CoA thioesterases involved in the biosynthesis of phylloquinone. It is noteworthy that neither of them correspond to the four plastid-targeted proteins that we had previously proposed as putative *Arabidopsis* DHNA-CoA thioesterases based on homology searches with the cyanobacterial enzyme (Slr0204; Widhalm *et al.*, 2009). Of those, three (*At1g68260*, *At1g35250* and *At1g35290*) fail to complement the *Synechocystis* DHNA-CoA thioesterase knock-out, and in fact are orthologous to recently characterized *Solanum lycopersicum* (tomato) methylketone synthases involved in the biosynthesis of 3-ketoacid volatiles (Yu *et al.*, 2010). The fourth one, *At1g68280*, a paralog of *At1g68260*, probably corresponds to a pseudogene.

DHNA-CoA thioesterase activity occurs in peroxisomes, thus establishing definitive evidence for a split of the phylloquinone biosynthetic pathway between this organelle and plastids. This arrangement is apparently not specific to *Arabidopsis*, for DHNA-CoA thioesterase activity is not detectable in plastids isolated from *Pisum sativum* (pea) seedlings either, one of the best sources for obtaining intact and highly pure chloroplasts (Cline, 1986), whereas it is readily measured in the initial whole extract (Table S4). In addition, orthologs of *AtDHNAT* in monocots, gymnosperms, mosses and Lycopodiophytes all display canonical peroxisomal targeting signals of type 1 (Figure S4). A tacit conclusion is that yet-to-be identified transport steps between plastids and peroxisomes are involved in the biosynthesis of phylloquinone. (Specifically for DHNA, an a priori reason against passive diffusion is the redox-active

**Figure 7.** Land-plant DHNA-CoA thioesterases are not of cyanobacterial descent.

(a) Non-exhaustive reconstruction of the structure-based maximum likelihood phylogeny of Slr0204-type, Paal-type and 4HBT-II-type hotdog-fold thioesterases using the MABL website (<http://www.phylogeny.fr>). PDB numbers of reference structures are given in brackets and alignments are provided in Figure S3. Full names and taxonomic origin of species, and protein accession numbers, are listed in Table S3. Red arrows point to enzymes for which there is experimental evidence of DHNA-CoA activity.

(b) Vitamin K biosynthetic gene clusters mined from the NCBI genomic database and SEED resources for comparative genomics (<http://the-seed.uchicago.edu/FIG/index.cgi>). Cyanobacterial, red algae and euglyphida gene clusters are modified from Widhalm *et al.* (2009). Matching colors and numbers indicate orthology. 1, DHNA-CoA thioesterase; 2, OSB-CoA ligase; 3, OSB synthase; 4, DHNA prenyltransferase; 5, isochorismate synthase; 6, SHCHC synthase; 7, DHNA-CoA synthase; 8, SEPHCHC synthase.



nature of its naphthoquinone ring. In other words, by freely shuttling through biological membranes, DHNA would act as an uncoupler and dissipate electrochemical gradients.) Extracts of the double mutant *atdhnat1 atdhnat2* still contain about 40% of the wild-type DHNA-CoA thioesterase activity, but the *atdhnat1* and *atdhnat2* T-DNA loci are not null. A detailed inspection of the *AtDHNAT1* sequence shows that an ATG codon (nucleotide position 49) located 19 nucleotides after the predicted T-DNA insertion of SAIL\_1253\_B02 could actually serve as an alternative start codon (Figure S5). Similarly, mining the NCBI cDNA database identifies an alternatively spliced version of the *AtDHNAT2* transcript (NM\_203182) containing an in-frame stop codon (nucleotide position 932) located 122 nucleotides before the

predicted T-DNA insertion of SAIL\_315\_C08 (Figure S5). Notably, both of the *atdhnat1* and *atdhnat2* alternative mRNAs would encode intact catalytic motifs (Figure S5). We also investigated the possibility that the gene *At5g48370*, which partially complements the *Synechocystis slr0204* knock-out mutant (Figure 2), encodes for an additional plant DHNA-CoA thioesterase. A cognate T-DNA knock-out line (SALK\_122483) was isolated, genotyped and confirmed by RT-PCR, but it did not display any statistically significant differences in phylloquinone content compared with wild-type *Arabidopsis* (Figure S6).

Besides invalidating their classification as Paal enzymes, a structure-adjusted phylogenetic reconstruction established plant DHNA-CoA thioesterases as new functional members

of the TE11/4HBT-II-type subfamily of hotdog-fold CoA thioesterases. That plant and cyanobacterial DHNA-CoA thioesterases display similar substrate specificity while having radically different catalytic sites exemplifies that, in the hotdog-fold superfamily, functions cannot be assigned on the basis of a mere comparison of primary sequences if the organisms are phylogenetically too distant. Most importantly, unlike their rhodophytes and euglyphidae counterparts, plant DHNA-CoA thioesterases are not of cyanobacterial ancestry. Instead, they are monophyletic with *Lactobacillales* orthologs that are encoded in clusters of vitamin K biosynthetic genes. It therefore seems very probable that the nuclear-encoded plant DHNA-CoA thioesterase originates from an event of horizontal gene transfer with a menaquinone-synthesizing bacterium of the *Lactobacillales* order. There is actually a similar precedent for this in plant phyloquinone biosynthesis with OSB-CoA ligase, which appears to have been directly acquired from a  $\delta$ -proteobacterium (Gross *et al.*, 2008). We therefore propose that the early plastid-containing common ancestor of rhodophytes, green algae and land plants bore a cyanobacterial DHNA-CoA thioesterase of the TE12/Slr0204 type. This gene would have been lost or have significantly diverged after the evolutionary split with red algae, as it is no longer detected in green algae and land plants. Green algae that do not appear to contain orthologs of the TE11/4HBT-II-type enzyme presumably possess a third type of DHNA-CoA thioesterase.

## EXPERIMENTAL PROCEDURES

### Chemicals and reagents

DHNA-CoA was synthesized as described in Widhalm *et al.* (2009). DHNA, benzoyl-CoA, phenylacetyl-CoA and menaquinone-4 were obtained from Sigma-Aldrich (<http://www.sigmaaldrich.com>). Phyloquinone was obtained from MP Biomedicals (<http://www.mpbio.com>). Unless otherwise mentioned, all other reagents were from Fisher Scientific (<http://www.fishersci.com>).

### Functional complementation of *synechocystis*

Arabidopsis cDNA clones G61320 (At1g48320), U89448 (At5g48950), G21545 (At3g61200), G12298 (At1g04290), G60738 (At2g29590), G13733 (At3g16175), G67253 (At5g48370), G67273 (At2g30720), U14083 (At1g68260), U84163 (At1g35250) and U14921 (At1g35290) were obtained from the Arabidopsis Biological Resource Center. No clone was available for At1g68280, and no corresponding cDNAs were amplified from total leaf RNA. Each cDNA was PCR-amplified for subcloning between the 5'-*Nde*I/3'-*Bam*HI, or for clone U89448 5'-*Nde*I/3'-*Bgl*II, sites of expression vector pSynExp-2 (Sattler *et al.*, 2003). A list of the corresponding primers used for the amplifications is provided in Table S2. All DNA constructs were verified by sequencing and were introduced into the *Synechocystis* *slr0204*: *Spec* knock-out mutant (Widhalm *et al.*, 2009), as described by Williams (1988). Transformed cells were selected for resistance to spectinomycin and chloramphenicol. Incorporation of cDNAs was verified by PCR on genomic DNA. Plates were incubated at 22°C with 30  $\mu\text{E m}^{-2} \text{s}^{-1}$ . For photosensitivity experiments, replicated plates containing no glucose or antibiotics were transferred at 150  $\mu\text{E m}^{-2} \text{s}^{-1}$ .

### Plant material and growth conditions

Arabidopsis T-DNA insertion lines SAIL\_1253\_B02 (At1g48320) and SAIL\_315\_C08 (At5g48950) were obtained from the Arabidopsis Biological Resource Center at the Ohio State University (<http://abr-c.osu.edu>). Seeds were allowed to germinate on Murashige-Skoog solid medium and were transferred to potting mix in a growth chamber at 22°C (100  $\mu\text{E m}^{-2} \text{s}^{-1}$ ) with 16-h days for 6 weeks. The double knock-out mutant was obtained by crossing individual homozygous mutants. For the preparation of chloroplasts and mitochondria, Arabidopsis seedlings (Col-0) were grown at 22°C (100  $\mu\text{E m}^{-2} \text{s}^{-1}$ ) with 10-h days for 2 weeks. For the isolation of peroxisomes, Arabidopsis plants were grown with 16-h days for 4 weeks.

### Plant genotyping and semiquantitative RT-PCR analyses

Arabidopsis plants were genotyped using the following primers: LP1, 5'-ATCCAATCCTCTGAAACCCTC-3', RP1, 5'-GTGCTTACAGGAGTTGCTTCG-3' (SAIL\_1253\_B02); LP2, 5'-CCATCCATTTGTATACCCGTG-3', RP2, 5'-TGTTTTGATGCAATATCGTGTG-3' (SAIL\_315\_C08); LP, 5'-GCTGGCATGTCAGAGAAAATC-3', RP, 5'-TCTTCACCCAACCATGAATTC-3' (SALK\_122483); and T-DNA specific primer LB2, 5'-GCTTCTATTATATCTTCCAAATACCAATACA-3' (SAIL lines) or LBB1, 5'-GCGTGGACCGCTTGCTGCAACT-3' (SALK line). Total RNA from Arabidopsis leaves were extracted using the SV Total RNA Isolation System (Promega, <http://www.promega.com>). PCR was performed on cDNAs prepared from 500 ng of total RNA using the following gene-specific primers: *AtDHNAT1*, 5'-CTTCTGTTTCTCCGTC-3' (RT1fwd) and 5'-CTACAACCTTTCGACCA TTT-3' (RT1rvs); *AtDHNAT2*, 5'-ATGGATCCAAATCGCCG-3' (RT2fwd) and 5'-CGCCGAATCTTTCCAGTCTC-3' (RT2rvs); *At5g48370*, 5'-GAATCTCTTCTCGATCCTCC-3' (RTfwd) and 5'-CCTTCTGTACCTCCTCTC-3' (RTrvs); actin control, 5'-CTAAGCTCAAGATCAAAGC-3' (forward) and 5'-TTAACATTGCAAAGAGTTTCAAGG-3' (reverse).

### Purification of Arabidopsis organelles

For the isolation of chloroplasts and mitochondria, 2-week-old Arabidopsis seedlings were de-starched for 18 h prior to tissue disruption. Chloroplasts were purified on a Percoll-gradient as described by Weigel and Glazebrook (2002), except that ascorbate and bovine serum albumin were omitted from the extraction and wash buffers. The procedure for the preparation of mitochondria was modified from Douce *et al.* (1987). For that, 13 g of leaves was homogenized in 75 ml of homogenization buffer (20 mM sodium pyrophosphate-HCl, pH 7.5, 1 mM EDTA, 300 mM mannitol) in a regular blender (three 5-s pulses). All steps were performed at 4°C. The homogenate was filtered through one layer of miracloth, and the remaining solid material was re-extracted with 25 ml of homogenization buffer. The filtrate was centrifuged (1500 **g** for 10 min), and the supernatant was collected to be re-centrifuged (10 000 **g** for 20 min). The resulting pellet was recovered and resuspended in 2 ml of sample buffer (10 mM HEPES-KOH, pH 7.2, 1 mM EDTA, 300 mM mannitol). The sample (2  $\times$  1 ml) was then layered over a discontinuous density gradient consisting of 60% (1.5 ml) and 28% (6 ml) of percoll prepared in sample buffer. After centrifugation (41 000 **g** for 40 min), the mitochondrial fractions (approximately 2  $\times$  1.5 ml) were collected at the interface of the percoll layers. Peroxisomes from wild-type Arabidopsis plants were prepared as described in Reumann *et al.* (2009), whereas those from the double *atdhnat1 dhnat2* knock-out mutant were prepared as described in Harrison-Lowe and Olsen (2006). Marker enzymes, glyceraldehyde-3-phosphate dehydrogenase (GAPDH), fumarase



and catalase were assayed as described by Oostende *et al.* (2008). For recovery and enrichment calculations, DHNA-CoA thioesterase activity was measured in the desalted crude extracts from the chloroplast preparation.

### Subcellular localization

Full-length *At5g48950* cDNA was subcloned into pK7WGF2 (Karimi *et al.*, 2002) using Gateway™ technology, resulting in an in-frame fusion with the C-terminal end of GFP. A KAT2-eqFP611 peroxisomal marker cassette, encoding for a C-terminal fusion of *Arabidopsis* 3-keto-acyl-CoA thiolase 2 (residues 1–99) with RFP under the control of the 35S promoter (Forner and Binder, 2007), was subcloned into the *EcoRI* and *PstI* sites of binary vector PZP212 (Hajdukiewicz *et al.*, 1994). 35S::GFP-*AtDHNAT2* and 35S::KAT2-eqFP611 constructs were individually electroporated into *Agrobacterium tumefaciens* C58C1, for subsequent co-infiltration into the leaves of *Nicotiana benthamiana*. Epidermal cells were imaged by confocal microscopy 2 days later.

### Preparation of Arabidopsis crude protein extracts

*Arabidopsis* leaves (0.75 g) were flash-frozen in liquid nitrogen and ground to a fine powder with pestle and mortar. The powder was transferred to a 40-ml screw-cap tube and thawed with 2.25 ml of 100 mM KH<sub>2</sub>PO<sub>4</sub>, pH 8.0, 5% (w/vol) polyvinylpyrrolidone and 5 mM freshly prepared DTT. Samples were centrifuged (10 000 *g* for 10 min at 4°C) to pellet debris. Supernatants were recovered and desalted on a PD-10 column equilibrated in 100 mM KH<sub>2</sub>PO<sub>4</sub> (pH 7.0), 5 mM DTT and 10% glycerol (vol/vol).

### Expression and purification of recombinant enzymes

*At1g48320* and *At5g48950* cDNAs were subcloned minus their stop codons using Gateway™ technology in expression vector pET-DEST42 (Invitrogen, <http://www.invitrogen.com>) for C-terminal fusion with a 6xHis tag. Constructs were introduced into *E. coli* BL21-CodonPlus (DE3)-RIL cells (Agilent, <http://www.home.agilent.com>). Starter cultures containing ampicillin were used to inoculate 500 ml of pre-warmed Luria–Bertani (LB) medium without antibiotic. When A<sub>600</sub> reached approximately 0.9, isopropyl-1-thio-β-D-galactopyranoside (500 μM) was added, and incubation was continued for 2 h at 30°C. Subsequent operations were at 4°C. Cells were harvested by centrifugation, resuspended in 8 ml of extraction buffer [50 mM NaH<sub>2</sub>PO<sub>4</sub> (pH 8.0), 300 mM NaCl, 10% glycerol (vol/vol) and 10 mM imidazole], and disrupted with 0.1-mm zirconia/silica beads in a MiniBeadbeater (BioSpec Products Inc., <http://www.biospec.com>) at 5000 rpm for 20 s, five times. The extracts were centrifuged (at 14 000 *g* for 10 min) and the recombinant proteins were purified under native conditions with Ni-NTA His-Bind resin (Novagen, <http://www.emdchemicals.com>), following the manufacturer's recommendations. Isolated proteins were immediately desalted on a PD-10 column (GE Healthcare, <http://www.gelifesciences.com>) equilibrated in 100 mM KH<sub>2</sub>PO<sub>4</sub> (pH 7.0), 10% glycerol (vol/vol). Desalted fractions were frozen in liquid N<sub>2</sub> and stored at –80°C.

### Enzyme assays

The DHNA-CoA thioesterase assays (50 μl) contained 100 mM KH<sub>2</sub>PO<sub>4</sub> (pH 7.0), 5 mM DTT, 35–90 μM DHNA-CoA and 0–49 μg of proteins, and were incubated in the dark for 10–20 min at 30°C. Negative controls containing boiled proteins and external standards of DHNA were incubated in parallel. Assays were terminated with the addition of 150 μl of ice-cold 95% ethanol (vol/vol). Samples were then centrifuged (at 16 000 *g* for 5 min at 8°C) and immediately analyzed by HPLC with fluorescence and diode array detection modules, as previously described (Widhalm *et al.*, 2009). The

hydrolysis of the benzoyl-CoA, phenylacetyl-CoA, palmitoyl-CoA and succinyl-CoA substrates was measured spectrophotometrically using the DTNB-derivatation method. Assays (375 μl) contained 100 mM KH<sub>2</sub>PO<sub>4</sub> (pH 7.0), 90 μM substrates and 0.65–2.7 μg of recombinant *AtDHNAT1* and 2. In addition, assays with palmitoyl-CoA contained 3 μM of BSA. Blank samples containing no enzyme or no substrate were included. Reactions were incubated for 60–180 min at 30°C, and were then mixed with 375 μl of an aqueous solution of 400 μM DTNB. Changes in A<sub>412</sub> compared with blank samples were read after a 5-minute incubation.

### Phylloquinone analyses

All steps were carried out in dimmed light to avoid the photo-degradation of naphthoquinone species. *Synechocystis* cells (1.8 ml) were harvested by centrifugation, and resuspended in 225 μl of BG-11 medium (Williams, 1988). Cells were quantified by absorbance at 730 nm using the formula 0.25 unit A<sub>730</sub> ⇔ 10<sup>8</sup> cells. A 150-μl aliquot was then added to 700 μl of 95% (vol/vol) ethanol and 220 μl of water into a pyrex screw-cap tube, spiked with 75 pmoles of menaquinone-4 as an internal standard. *Arabidopsis* leaves (8–21 mg fresh weight) were spiked with 150 pmoles of menaquinone-4 as an internal standard, and were homogenized in 1 ml of 100% (vol/vol) methanol using a pyrex tissue grinder. The extract was then transferred to a pyrex tube containing 0.6 ml of water. *Synechocystis* and *Arabidopsis* extracts were then partitioned with 5 ml of hexane. Upper phases were transferred into a new tube, and then evaporated to dryness under a gentle stream of gaseous N<sub>2</sub>. The residue was redissolved into 200 μl of ethanol. The samples (100 μl) were analyzed by HPLC on a 5 μM Supelco Discovery C-18 column (250 × 4.6 mm, Sigma-Aldrich), thermostated at 30°C and eluted in isocratic mode at a flow rate of 1 ml min<sup>-1</sup> with methanol : ethanol (80 : 20 vol/vol), containing 1 mM sodium acetate, 2 mM acetic acid and 2 mM ZnCl<sub>2</sub>. Naphthoquinone species were detected fluorometrically (at 238 and 426 nm for excitation and emission, respectively) after reduction into a post-column chemical reactor (70 × 1.5 mm) packed with –100 mesh zinc powder (Sigma-Aldrich). Phylloquinone and menaquinone-4 were quantified according to external calibration standards, and data were corrected for the recovery of the internal standard.

### ACKNOWLEDGEMENTS

This work was made possible in part by National Science Foundation Grant MCB-0918258 (to GJB), support from the Center for Plant Science Innovation, and a graduate research assistantship from the Department of Agronomy and Horticulture at UNL (to JRW). We thank Dr Nicola Harrison-Lowe for her assistance with the preparation of peroxisomes, Dr Anna K. Block for her assistance with the subcloning of the KAT2-eqFP611 cassette and Dr Guodong Ren for his assistance with the making of the *Arabidopsis* double knock-out mutant.

### SUPPORTING INFORMATION

Additional Supporting Information may be found in the online version of this article:

**Figure S1.** The biosynthetic pathway of phylloquinone.

**Figure S2.** Expression and purification of recombinant *AtDHNAT1* and *AtDHNAT2*.

**Figure S3.** Phenotypes of wild-type, *atdhnat1 AtDHNAT2*, *AtDHNAT1 atdhnat2* and *atdhnat1 atdhnat2* *Arabidopsis* plants.

**Figure S4.** Sequence alignment of prokaryotic and eukaryotic DHNA-CoA thioesterases and related proteins.

**Figure S5.** Schemes of the *atdhnat1* and *atdhnat2* loci.

**Figure S6.** Molecular characterization of *At5g48370* T-DNA insertion mutant (SALK\_122483) and phyloquinone analyses.

**Table S1.** DHNA-CoA thioesterase activity of *Escherichia coli* crude extracts.

**Table S2.** Primer sets used for the subcloning of Arabidopsis cDNA clones in expression vector pSynExp-2.

**Table S3.** Accession numbers and taxonomic origin of proteins used for phylogenetic reconstruction.

**Table S4.** DHNA-CoA thioesterase activity in pea seedling crude extracts and percoll-purified chloroplasts.

Please note: As a service to our authors and readers, this journal provides supporting information supplied by the authors. Such materials are peer-reviewed and may be re-organized for online delivery, but are not copy-edited or typeset. Technical support issues arising from supporting information (other than missing files) should be addressed to the authors.

## REFERENCES

- Babujee, L., Wurtz, V., Ma, C., Lueder, F., Soni, P., van Dorselaer, A. and Reumann, S. (2010) The proteome map of spinach leaf peroxisomes indicates partial compartmentalization of phyloquinone (vitamin K1) biosynthesis in plant peroxisomes. *J. Exp. Bot.* **61**, 1441–1453.
- Benning, M.M., Wesenberg, G., Liu, R., Taylor, K.L., Dunaway-Mariano, D. and Holden, H.M. (1998) The three-dimensional structure of 4-hydroxybenzoyl-CoA thioesterase from *Pseudomonas* sp. strain CBS-3. *J. Biol. Chem.* **273**, 33572–33579.
- Booth, S.L. (2009) Roles for vitamin K beyond coagulation. *Annu. Rev. Nutr.* **29**, 89–110.
- Booth, S.L. and Suttie, J.W. (1998) Dietary intake and adequacy of vitamin K. *J. Nutr.* **128**, 785–788.
- Brettel, K., Sétif, P. and Mathis, P. (1986) Flash-induced absorption changes in photosystem I at low temperature: evidence that the electron acceptor A1 is vitamin K1. *FEBS Lett.* **203**, 220–224.
- Cantu, D.C., Chen, Y. and Reilly, P.J. (2010) Thioesterases: a new perspective based on their primary and tertiary structures. *Protein Sci.* **19**, 1281–1295.
- Cantu, D.C., Chen, Y., Lemons, M.L. and Reilly, P.J. (2011) ThYme: a database for thioester-active enzymes. *Nucleic Acids Res.* **39**, D342–D346.
- Cline, K. (1986) Import of proteins into chloroplasts. membrane integration of a thylakoid precursor protein reconstituted in chloroplast lysates. *J. Biol. Chem.* **261**, 14804–14810.
- Collins, M.D. and Jones, D. (1981) Distribution of isoprenoid quinone structural types in bacteria and their taxonomic implication. *Microbiol. Rev.* **45**, 316–354.
- Dillon, S.C. and Bateman, A. (2004) The hotdog fold: wrapping up a superfamily of thioesterases and dehydratases. *BMC Bioinformatics*, **5**, 109.
- Douce, R., Bourguignon, J., Brouquisse, R. and Neuburger, M. (1987) Isolation of plant mitochondria: general principles and criteria of integrity. *Methods Enzymol.* **148**, 403–415.
- Finn, R.D., Mistry, J., Tate, J. et al. (2010) The pfam protein families database. *Nucleic Acids Res.* **38**, D211–D222.
- Forner, J. and Binder, S. (2007) The red fluorescent protein eqFP611: application in subcellular localization studies in higher plants. *BMC Plant Biol.* **7**, 28.
- Furt, F., Oostende, C., Widhalm, J.R., Dale, M.A., Wertz, J. and Basset, G.J. (2010) A bimodular oxidoreductase mediates the specific reduction of phyloquinone (vitamin K) in chloroplasts. *Plant J.* **64**, 38–46.
- Garcion, C., Lohmann, A., Lamodié, E., Catinot, J., Buchala, A., Doermann, P. and Metraux, J.P. (2008) Characterization and biological function of the ISOCHORISMATE SYNTHASE2 gene of arabidopsis. *Plant Physiol.* **147**, 1279–1287.
- Gaullière, J., d'Harlingue, A., Camara, B. and Monéger, R. (1984) Prenylation and methylation reactions in phyloquinone (vitamin K<sub>1</sub>) synthesis in *capsicum annuum* plastids. *Plant Cell Rep.* **3**, 240–242.
- Gross, J., Cho, W.K., Lezhneva, L., Falk, J., Krupinska, K., Shinozaki, K., Seki, M., Herrmann, R.G. and Meurer, J. (2006) A plant locus essential for phyloquinone (vitamin K1) biosynthesis originated from a fusion of four eubacterial genes. *J. Biol. Chem.* **281**, 17189–17196.
- Gross, J., Meurer, J. and Bhattacharya, D. (2008) Evidence of a chimeric genome in the cyanobacterial ancestor of plastids. *BMC Evol. Biol.* **8**, 117.
- Hajdukiewicz, P., Svab, Z. and Maliga, P. (1994) The small, versatile pPZP family of agrobacterium binary vectors for plant transformation. *Plant Mol. Biol.* **25**, 989–994.
- Harrison-Lowe, N. and Olsen, L.J. (2006) Isolation of glyoxysomes from pumpkin cotyledons. *Curr Protoc Cell Biol.* Chapter 3: Unit 3.19.
- Ikeda, Y., Komura, M., Watanabe, M., Minami, C., Koike, H., Itoh, S., Kashino, Y. and Satoh, K. (2008) Photosystem I complexes associated with fucoxanthin-chlorophyll-binding proteins from a marine centric diatom, *Chaetoceros gracilis*. *Biochim. Biophys. Acta.* **1777**, 351–361.
- Jiang, M., Chen, X., Guo, Z.F., Cao, Y., Chen, M. and Guo, Z. (2008) Identification and characterization of (1R,6R)-2-succinyl-6-hydroxy-2,4-cyclohexadiene-1-carboxylate synthase in the menaquinone biosynthesis of *Escherichia coli*. *Biochemistry*, **47**, 3426–3434.
- Kaipig, S., Soll, J. and Schultz, G. (1984) Site of methylation of 2-phytyl-1,4-naphthoquinol in phyloquinone (vitamin K1) synthesis in spinach chloroplasts. *Phytochemistry*, **23**, 89.
- Karamoko, M., Cline, S., Redding, K., Ruiz, N. and Hamel, P.P. (2011) Lumen thiol oxidoreductase1, a disulfide bond-forming catalyst, is required for the assembly of photosystem II in Arabidopsis. *Plant Cell*, **23**, 4462–4475.
- Karimi, M., Inze, D. and Depicker, A. (2002) GATEWAY vectors for agrobacterium-mediated plant transformation. *Trends Plant Sci.* **7**, 193–195.
- Kim, H.U., van Oostende, C., Basset, G.J. and Browse, J. (2008) The AAE14 gene encodes the arabidopsis o-succinylbenzoyl-CoA ligase that is essential for phyloquinone synthesis and photosystem-I function. *Plant J.* **54**, 272–283.
- Lohmann, A., Schottler, M.A., Brehelin, C., Kessler, F., Bock, R., Cahoon, E.B. and Dormann, P. (2006) Deficiency in phyloquinone (vitamin K1) methylation affects prenyl quinone distribution, photosystem I abundance, and anthocyanin accumulation in the arabidopsis AtmenG mutant. *J. Biol. Chem.* **281**, 40461–40472.
- Oostende, C., Widhalm, J.R. and Basset, G.J. (2008) Detection and quantification of vitamin K(1) quinol in leaf tissues. *Phytochemistry*, **69**, 2457–2462.
- Reumann, S. (2004a) Specification of the peroxisome targeting signals type 1 and type 2 of plant peroxisomes by bioinformatics analyses. *Plant Physiol.* **135**, 783–800.
- Reumann, S., Ma, C., Lemke, S. and Babujee, L. (2004b) AraPerox. A database of putative arabidopsis proteins from plant peroxisomes. *Plant Physiol.* **136**, 2587–2608.
- Reumann, S., Babujee, L., Ma, C., Wienkoop, S., Siemsen, T., Antonicelli, G.E., Rasche, N., Luder, F., Weckwerth, W. and Jahn, O. (2007) Proteome analysis of arabidopsis leaf peroxisomes reveals novel targeting peptides, metabolic pathways, and defense mechanisms. *Plant Cell*, **19**, 3170–3193.
- Reumann, S., Quan, S., Aung, K. et al. (2009) In-depth proteome analysis of arabidopsis leaf peroxisomes combined with *in vivo* subcellular targeting verification indicates novel metabolic and regulatory functions of peroxisomes. *Plant Physiol.* **150**, 125–143.
- Sakuragi, Y. and Bryant, D.A. (2006) Genetic manipulation of quinone biosynthesis in cyanobacteria. In *Advances in Photosynthesis and Respiration. Photosystem I: The light-Driven Plastocyanin: Ferredoxin Oxidoreductase in Photosynthesis* (Golbeck, J.H., ed.). Dordrecht, The Netherlands: Springer, pp. 205–222.
- Sattler, S.E., Cahoon, E.B., Coughlan, S.J. and DellaPenna, D. (2003) Characterization of tocopherol cyclases from higher plants and cyanobacteria. evolutionary implications for tocopherol synthesis and function. *Plant Physiol.* **132**, 2184–2195.
- Schultz, G., Soll, J. and Ellerbrock, B.H. (1981) Site of prenylation reaction in synthesis of phyloquinone (vitamin K1) by spinach chloroplasts. *Eur. J. Biochem.* **117**, 329–332.
- Sessions, A., Burke, E., Presting, G. et al. (2002) A high-throughput arabidopsis reverse genetics system. *Plant Cell*, **14**, 2985–2994.
- Shimada, H., Ohno, R., Shibata, M., Ikegami, I., Onai, K., Ohto, M.A. and Takamiya, K. (2005) Inactivation and deficiency of core proteins of photosystems I and II caused by genetical phyloquinone and plastoquinone deficiency but retained lamellar structure in a T-DNA mutant of arabidopsis. *Plant J.* **41**, 627–637.
- Sigfridsson, K., Hansson, O. and Brzezinski, P. (1995) Electrogenic light reactions in photosystem I: resolution of electron-transfer rates between the iron-sulfur centers. *Proc. Natl Acad. Sci. USA*, **92**, 3458–3462.
- Singh, A.K., Bhattacharyya-Pakrasi, M. and Pakrasi, H.B. (2008) Identification of an atypical membrane protein involved in the formation of protein

- disulfide bonds in oxygenic photosynthetic organisms. *J. Biol. Chem.* **283**, 15762–15770.
- Strawn, M.A., Marr, S.K., Inoue, K., Inada, N., Zubieta, C. and Wildermuth, M.C.** (2007) Arabidopsis isochorismate synthase functional in pathogen-induced salicylate biosynthesis exhibits properties consistent with a role in diverse stress responses. *J. Biol. Chem.* **282**, 5919–5933.
- Thoden, J.B., Holden, H.M., Zhuang, Z. and Dunaway-Mariano, D.** (2002) X-ray crystallographic analyses of inhibitor and substrate complexes of wild-type and mutant 4-hydroxybenzoyl-CoA thioesterase. *J. Biol. Chem.* **277**, 27468–27476.
- Weigel, D. and Glazebrook, J.** (2002) *Arabidopsis: A laboratory manual*. New York, USA: Cold Spring Harbor Laboratory Press.
- Widhalm, J.R., van Oostende, C., Furt, F. and Basset, G.J.** (2009) A dedicated thioesterase of the hotdog-fold family is required for the biosynthesis of the naphthoquinone ring of vitamin K1. *Proc. Natl Acad. Sci. USA*, **106**, 5599–5603.
- Williams, J.G.K.** (1988) Construction of specific mutations in photosystem II photosynthetic reaction center by genetic engineering methods in *synechocystis* 6803. *Methods Enzymol.* **167**, 766–778.
- Yoshida, E., Nakamura, A. and Watanabe, T.** (2003) Reversed-phase HPLC determination of chlorophyll a' and naphthoquinones in photosystem I of red algae: existence of two menaquinone-4 molecules in photosystem I of cyanidium caldarium. *Anal. Sci.* **19**, 1001–1005.
- Yu, G., Nguyen, T.T.H., Guo, Y. et al.** (2010) Enzymatic functions of wild tomato methylketone synthases 1 and 2. *Plant Physiol.* **154**, 67–77.